Distinct neural representations of hand movement direction between motor imagery and execution in the presupplementary motor area

Yuxiang Yang[a], Huixiang Yang[b], Fumihito Imai[a], Kenji Ogawa[a*]

[a]Department of Psychology, Graduate School of Humanities and Human Sciences, Hokkaido University

[b]Institute for Advanced Co-Creation Studies, Osaka University

*Corresponding author:

Dr. Kenji Ogawa

Department of Psychology, Graduate School of Humanities and Human Sciences, Hokkaido University, Kita 10, Nishi 7, Kita-ku, Sapporo, 060-0810 Japan

Tel/Fax: +81-011-706-4093

E-mail: ogawa@let.hokudai.ac.jp.

Total number of pages: 25

Total number of figures: 7

Total number of tables: 3

Abstract

Motor simulation theory proposes a functional equivalence between motor execution (ME) and its simulation, suggesting that motor imagery (MI) is the self-intentioned simulation of one's actions. This study used functional magnetic resonance imaging (fMRI) with multivoxel pattern analysis to test whether the direction of hand movement is represented with a similar neural code between ME and MI. In our study, participants used their right hand to move an on-screen cursor in the left–right direction with a joystick or imagined the same movement without execution. The results indicated that the left–right direction as well as their modality (ME or MI) could be decoded significantly above the chance level in the presupplementary motor area (pre-SMA) and primary visual cortex (V1). Next, we used activation patterns of ME as inputs to the decoder to predict hand move directions in MI sessions and found a significantly higher-than-chance accuracy only in V1, not in pre-SMA. Moreover, the representational similarity analysis showed similar activation patterns for the same directions between ME and MI in V1 but not in pre-SMA. This study's finding indicates distinct spatial activation patterns for movement directions between ME and MI in pre-SMA.

Keywords

motor imagery; motor execution; fMRI; multivoxel classification analysis; representational similarity analysis; presupplementary motor area

Introduction

Motor imagery (MI) is a cognitive ability defined as a "mental simulation" of motor execution (ME) without actual action (Decety, 1996; Grush, 2004; Hanakawa, 2016). It has been believed that the neural state of an imagined movement is similar to the state of execution of that action (Jeannerod, 2001). Early neuroimaging studies showed that MI and ME activate roughly the same brain regions (Hanakawa et al., 2008; Munzert et al., 2009). Moreover, a large overlap of regions between MI and ME was found in a meta-analysis study (Hardwick et al., 2018). However, these studies mainly analyzed a single voxel activity or averaged activities within the region and not the activation patterns among multivoxels. Thus, although MI and ME could activate the same brain regions, it remains unclear whether MI and ME use similar neural codes for the same action.

Recently, a technique called multivoxel pattern analysis (MVPA) was developed (Weaverdyck et al., 2020). MVPA examines the spatial pattern of brain activations, whereas univariate analyses only consider the overall magnitude of the responses. MVPA studies showed that MI for different types of right-hand actions could be decoded significantly above chance level in M1 and premotor cortices (Pilgramm et al., 2016). Moreover, these different hand actions could also be decoded between MI and ME (cross-model) in premotor cortices. However, in representational similarity analysis (RSA), representational dissimilarity matrices showed that MI and ME represent separate clusters, although the representational organization of action types within these clusters was identical (Zabicki et al., 2017). Therefore, premotor cortices use similar neural codes for different types of hand actions between MI and ME.

By contrast, it remains unclear whether the different directions of specific hand

action use the same neural code between MI and ME. Ogawa and Inui instructed the participants to perform visually guided movements using a normal mouse and a left–right reversed mouse. Their study showed that the direction of hand movement could be decoded in the hand region of the primary motor area (Mot) (Ogawa & Inui, 2012). Our study thus attempted to decode ME of hand movement direction and investigate whether we could decode MI in motor-related regions.

Our study also examined whether the same hand movement, but with different directions in MI and ME used similar neural codes. Our participants first performed the ME tasks by moving their right hand using a joystick to move an invisible cursor to the left or right target. They subsequently performed the MI tasks, imagining the same action as the ME tasks. This experimental design allowed us to compare the activity pattern between ME and MI using multivoxel classification analysis and RSA.

Materials and Methods

Participants

Participants were 17 volunteers (12 females, 5 males) from Hokkaido University, with an average age of 23.18 years (range = 20–26, SD = 1.74). Of these, two female participants were excluded because of excessive head movement during scanning. All participants were right-handed, according to the Edinburgh Handedness Inventory. The sample size was estimated from a prior hand-moving decoding study (Ogawa & Inui, 2012) using G*Power version 3.1.9 (Erdfelder et al., 2009; Faul et al., 2007). We used 15 participants to get power $(1 - \beta) = .95$, with $\alpha = .05$ and Cohen's $d = 1.03$.

Task procedures

All participants completed two practice sessions containing ten trials before three ME sessions and three MI sessions (20 trials per ME and MI session) in a functional magnetic resonance imaging (fMRI) scanner without scanning. Experimental stimuli were controlled by Psychophysics Toolbox Version 3 (PTB-3) (Brainard, 1997; Kleiner et al., 2007; Pelli, 1997) in MATLAB (The MathWorks, Inc.).

Practice session

In practice session 1, for each trial, a white fixation was presented in the center of the screen, and above the fixation, there was a countdown from "3" to "1" that lasted 3 s. At the end of the countdown, two squares were presented on the left and right sides of the screen, and the color of the central fixation changed to green or yellow (target phase), indicating the target (green: left square; yellow: right square). Half of the ten trials were green, and the other half was yellow, presented in random order. After 2 s, the color of central fixation changed to red (execution phase). During the execution phase, a joystick cursor (a small white "x") was presented centrally on the screen. The participants then moved the cursor with their right hand to the target square, which was indicated in the target phase, and maintained the cursor in the target square until the color of the central fixation changed from red to white. The execution phase lasted for 2 s, and then, the cursor was frozen, showing the participants the final position of the cursor in the execution phase for 3 s (result phase). Participants then allowed the joystick to return to its original position and let the joystick bring their right hand back (Figure 1). Participants repeated practice session 1 until getting 100% accuracy. Practice session 2 is almost the same as practice session 1. The difference was that in the execution phase of practice session 2, the joystick cursor was not presented. Moreover, it showed the

cursor's last position in the execution phase to the participants in the result phase.

Execution session

During the execution sessions, participants completed three execution sessions with fMRI scanning. The differences between execution sessions and practice session 2 were that each execution session included 20 trials (half were left, and half were right), and the time of countdown in the countdown phase was from 3 to 9 s (Figure 2).

Imagery session

After three execution sessions, participants completed three imagery sessions (20 trials per session). In the imagery session, the execution phase changed to the imagery phase, and the result phase changed to the evaluation phase with the same duration. In the imagery phase, participants imagined that they move the cursor by using the joystick and put the cursor into the target, which was indicated in the target phase, without actual movement. Participants were instructed to use both kinesthetic and visual images before the practice session. After the imagery phase, the participants immediately evaluated the quality of the MI in this trial using their left hand (from 1: very good to 4: very poor). In the evaluation phase, participants were instructed only to choose "4" when they failed to imagine before the practice session, which helped us to exclude the error.

MRI acquisition

"All scans were performed on a Siemens (Erlangen, Germany) 3-Tesla Prisma scanner with a 64-channel head coil at Hokkaido University. T2*-weighted echo-planar imaging (EPI) was used to acquire a total of 170 scans per session, with a gradient EPI sequence.

The first three scans within each session were discarded to allow for T1 equilibration. The scanning parameters were repetition time (TR), 2000 ms; echo time (TE), 30 ms; flip angle (FA), 90°; field of view (FOV), 192 × 192 mm; matrix, 94 × 94; 35 axial slices; and slice thickness, 3.0 mm with a 0.75 mm gap. T1-weighted anatomical imaging with an MP-RAGE sequence was performed using the following parameters: TR, 2300 ms; TE, 2.41 ms; FA, 8°; FOV; 256 × 256 mm; matrix, 256 × 256; 224 axial slices; and slice thickness, 0.8 mm without a gap.

Exclusion criteria for data

For more accurate data analysis, we excluded some fMRI data based on the behavioral criteria below.

a. The trial in which the participant moved the joystick before the execution phase in execution sessions.

b. The trial in which the participant did not put the cursor in the target square at the end of the execution phase in execution sessions.

c. The trial in which the participant moved the joystick to the wrong direction in execution sessions, although the cursor was in the correct target square at the end of the execution phase.

d. The trial in which participants chose “4 very poor” in the evaluation phase of imagery sessions.

Definition of regions of interest (ROIs)

We defined motor-related regions as bilateral pre-SMA, SMA, and left M1, PMv using Human Motor Area Template (Mayka et al., 2006), and left V1 was defined as

Brodmann Area 17. The activity of the left M1 reflected the movement of the right hand, whereas the direction of movement of the right hand can also be classified in the left M1 (Ogawa & Inui, 2012). SMA and premotor cortex were associated with MI (Decety, 1996). Furthermore, PMv was related to hand actions (Rizzolatti et al., 2002). Pre-SMA was also related to MI (Hanakawa et al., 2003), and pre-SMA was activated when the cursor was unavailable during visual guided movement (Ogawa et al., 2006; Ogawa & Inui, 2007).

fMRI mass-univariate analysis

Image preprocessing was performed using the SPM12 software (Welcome Department of Cognitive Neurology, http://www.fil.ion.ucl.ac.uk/spm). All functional images were initially realigned to adjust for motion-related artifacts. Volume-based realignment was performed by co-registering images using rigid body transformation to minimize the squared differences between volumes. The realigned images were then spatially normalized with the Montreal Neurological Institute template based on the affine and nonlinear registration of coregistered T1-weighted anatomical images (normalization procedure of SPM). They were resampled into 3-mm-cube voxels with the sinc interpolation. Images were spatially smoothed using a Gaussian kernel of 6 × 6 × 6-mm full width at half-maximum. However, images used for MVPA were not smoothed to avoid blurring the fine-grained information contained in the multivoxel activity (Kamitani & Sawahata, 2010; Mur et al., 2009; Ogawa et al., 2019). We analyzed significantly activated areas during the ME or MI of right-hand movement compared with activation during rest with univoxel analysis. Activation was the threshold at $p < .05$, corrected for multiple comparisons for a family-wise error, with an extent

threshold of 10 voxels.

Multivoxel pattern analysis

In decoding analysis of MVPA, we classified the direction of hand movement in ME and MI. The classification was performed based on a linear support vector machine run by LIBSVM (http://www.csie.ntu.edu.tw/~cjlin/libsvm) with a fixed regularization parameter C = 1. The beta value for each trial of voxels within ROIs (see Table 1) was used as inputs to the classifier. ROI size did not affect the linear SVM's decoding accuracy (Misaki et al., 2010). We attempted to interpret the direction of hand movement in only ME (ME classification) or MI (MI classification) and between ME and MI (cross-classification). Each participant attended three ME sessions and three MI sessions. In ME classification and MI classification, we estimated the average classification accuracy by a three-fold "leave-one-out" cross-validation, in which two sessions were used as training and the remaining session was used as test data. In cross-classification, the averaged classification accuracy was estimated via validation between three ME sessions and three MI sessions (Table 2). Such cross-classification between different task sets or stimuli has been used to investigate the activation pattern similarities (Ogawa & Imai, 2016).

To compare spatial activation pattern similarities for different directions across ME and MI, RSA (Kriegeskorte et al., 2008) was also conducted. Beta values of voxels within ROIs were used as inputs to estimate the representational dissimilarity matrix among the different directions of hand movement between ME and MI. There were a total of 30 trials for each direction and modality (3 sessions × 10 trials). Dissimilarity was measured with cross-validated Mahalanobis distance (Ejaz et al., 2015), which

presents reliable dissimilarity metrics for RSA (Walther et al., 2016). To ensure invertibility and stability, the voxel-by-voxel noise covariance matrix was separately estimated within one dataset using an optimal shrinkage algorithm (Ledoit & Wolf, 2003). We then compared the off-diagonal elements of the representational dissimilarity matrix, which represent the dissimilarity of activation patterns between different modalities and directions.

Results

Behavioral analysis

According to the exclusion criteria, we excluded the error trials based on behavior data. In a total of 60 trials of ME sessions and 60 trials of MI sessions, the percentage (SD) of error trials per participant in ME and MI sessions was 2.78% (3.77%) and 2.12% (3.18%), respectively.

fMRI mass-univariate analysis

We analyzed the activated regions of the brain using a univariate analysis of single voxels and the regions that were significantly activated by comparing the modalities (ME vs. MI) and the direction of movements (left vs. right). Activities between the left–right directions in ME were compared. No areas significantly differed between the left and right directions in ME at the corrected threshold of $p < .05$ and an extent threshold of 10 voxels. Both left and right directions of the right hand moving revealed the activations in the left M1 and left insula (Figure 3 and Table 3). Next, we compared the activity during which the participants imagined the right hand moving between the left and right directions. This comparison also revealed that no areas were significantly

differently activated between the left and right directions in MI. Both left and right directions of hand-moving imagery revealed the activations in the bilateral insula and SMA (Figure 3). Next, we compared the activated regions between the ME sessions and the MI sessions. Activations were found to be majorly in the left M1 and vermis during ME sessions and right M1 during MI sessions. There were no overlapped areas between "ME > rest" and "MI > rest" at the corrected threshold of $p < .05$ and an extent threshold of 10 voxels (Figure 4).

Next, ROI analysis was performed to compare the averaged parameter estimates (beta values) between the ME and MI sessions and the left and right directions. Repeated measures analysis of variance was conducted with the modalities (ME and MI) and the hand movement directions (left and right) as within the subjects' factors (Figure 5). In both left M1 and bilateral SMA, a significant main effect was observed between the ME and MI (left M1, $F(1, 14) = 43.791$, $p < .001$, $\mu_p^2 = .758$; bilateral SMA, $F(1, 14) = 8.569$, $p = .011$, $\mu_p^2 = .380$) and also a significant interaction between the two factors (left M1, $F(1, 14) = 11.274$, $p = .005$, $\mu_p^2 = .446$; bilateral SMA, $F(1, 14) = 13.074$, $p = .003$, $\mu_p^2 = .483$). The beta value of the left M1 and bilateral SMA was significantly higher when the hand was moving to the left than the right in ME sessions (left M1, $F = 8.132$, $p = .013$; bilateral SMA, $F = 12.149$, $p = .004$). In bilateral pre-SMA, there was no main effect but a significant interaction was observed ($F(1, 14) = 8.375$, $p = .012$, $\mu_p^2 = .374$). In the right direction, the beta value of bilateral pre-SMA in the MI sessions was significantly higher than in the ME sessions ($F = 5.134$, $p = .040$). Also, in the ME sessions, the beta value of bilateral pre-SMA was significantly higher when the hand was moving to the left than the right ($F = 11.759$, $p = .004$).

Multivoxel classification analysis

We first conducted MVPA to classify the direction of ME by the subjects using the activities of each ROI. In left M1, significantly higher-than-chance classification accuracy was observed ($t(14) = 6.49$, $p < .001$, Cohen's $d = 1.68$). We also found significantly higher-than-chance classification accuracies in bilateral pre-SMA ($t(14) = 3.38$, $p = .005$, Cohen's $d = .87$), SMA($t(14) = 2.61$, $p = .021$, Cohen's $d = .67$), and left PMv ($t(14) = 2.42$, $p = .030$, Cohen's $d = .62$), V1 ($t(14) = 11.89$, $p < .001$, Cohen's $d = 3.07$) (Figure 6A). Next, we conducted MVPA to classify the direction of MI. We found significantly higher-than-chance classification accuracies in bilateral pre-SMA ($t(14) = 2.61$, $p = .010$, Cohen's $d = .77$) and left V1 ($t(14) = 3.29$, $p = .005$, Cohen's $d = .85$), but no significant difference in bilateral SMA ($t(14) = -.87$, $p = .398$, Cohen's $d = -.23$) and left M1 ($t(14) = 1.13$, $p = .277$, Cohen's $d = .29$), PMv ($t(14) = 1.07$, $p = .304$, Cohen's $d = .28$) (Figure 6B).

We also conducted MVPA to classify the direction across ME and MI. We found significantly higher-than-chance classification accuracies in left V1 ($t(14) = 5.87$, $p < .001$, Cohen's $d = 1.52$). However, no significant difference in bilateral pre-SMA ($t(14) = .44$, $p = .665$, Cohen's $d = .11$), SMA ($t(14) = -.15$, $p = .883$, Cohen's $d = -.04$) and left M1 ($t(14) = .95$, $p = .358$, Cohen's $d = .25$), PMv ($t(14) = .31$, $p = .763$, Cohen's $d = .08$) (Figure 6C). These results indicated distinct spatial activation patterns for the movement directions between ME and MI in pre-SMA.

Representational similarity analysis

The RSA was used to investigate similarity in activation patterns of bilateral pre-SMA

and left V1 between different directions (left vs. right) across modalities (ME and MI, Figure 7A). Because bilateral pre-SMA and left V1 were the only ROIs that were significantly higher-than-chance in the ME classification and MI classification, a paired sample t-test was conducted with the dissimilarity between the same direction but different modalities (e.g., ME left and MI left) and different directions with different modalities (e.g., ME left and MI right) across ME and MI for bilateral pre-SMA and left V1 (Figure 7B). The result showed that different direction dissimilarities across ME and MI was significantly higher than the dissimilarity of the same direction in left V1 with null hypothesis significance testing, whereas there was no evidence for a difference between the dissimilarities by Bayes factor ($t(29) = 2.06$, $p = .049$, Cohen's $d = .376$, $BF_{10} = 1.221$). There was moderate evidence for no difference between the dissimilarity of different directions across modalities and the dissimilarity of same direction across modalities in bilateral pre-SMA ($t(29) = .33$, $p = .745$, Cohen's $d = .060$, $BF_{10} = .204$).

Discussion

This study investigated whether the different hand movement directions shared a similar neural code in motor-related regions between ME and MI. We first analyzed activated regions in the whole brain with conventional univoxel analysis within the ME and MI sessions. During the execution phase of the ME session, significantly increased activations were found in left M1 and left insula in both left and right directions. The left M1 is well known for its role in right-hand movements (Sanes et al., 1995). Contralateral insula activation has also been reported during voluntary limb movement (Chollet et al., 1991) and finger movements (Fink et al., 1997). During the imagery phase of the MI session, both left and right directions of hand moving imagery revealed

the activations in bilateral insula and SMA. A previous study indicated that SMA activity was associated with MI (Decety, 1996). The comparison between left and right direction hand movements in both ME and MI sessions showed no significant activated areas. This result indicated that conventional univoxel analysis could not distinguish differences in brain activity between the left and right directions of hand movements in both ME and MI.

ROI analysis of the beta value revealed that left M1, SMA, and pre-SMA activities were significantly higher during right hand moving to the left direction than the right direction in ME sessions. The previous study showed that right hands that were rotated in a clockwise direction were more difficult than when they were rotated in a counterclockwise direction (de Lange et al., 2006). That might cause stronger activities in left M1, SMA, and pre-SMA during the movement of the right hand to the left side.

Our multivoxel classification analysis in ME classification revealed that the classification accuracies in bilateral SMA, pre-SMA, and left M1, PMv, and V1 were significantly higher than the chance level. The left M1 and V1 result is consistent with the previous study (Ogawa & Inui, 2012), which also classified the hand movement directions while participants used a mouse. Bilateral SMA is associated with the preparation and readiness for voluntary movements (Cunnington et al., 1996, 2003), whereas PMv is related to hand actions (Rizzolatti et al., 2002). Pre-SMA is related to visuomotor imagery (Deiber et al., 1998; Johnston et al., 2004; Leek & Johnston, 2009). Previous studies showed that pre-SMA activates when visual feedback is unavailable during visual guided movements (Ogawa et al., 2006; Ogawa & Inui, 2007). In the present study, there was no visual feedback during ME sessions, the participants might visually estimate cursor position during right-hand movement. Our multivoxel

classification analysis in MI classification revealed that significantly higher-than-chance classification accuracy occurred only in bilateral pre-SMA and left V1, which showed that V1 and pre-SMA were also related to hand movement direction in MI.

We conducted cross-classification to investigate whether the different hand movement directions between ME and MI shared a similar neural code in bilateral pre-SMA and left V1. We only found significantly higher-than-chance accuracy in left V1, not in the bilateral pre-SMA. This result suggests that the activation of pre-SMA, although related to both ME and MI, and the activity patterns in pre-SMA are separate from each other. We conducted RSA to confirm this result further. The result of RSA showed that the dissimilarity of different directions across ME and MI was significantly higher than the dissimilarity of the same direction in left V1, and there was moderate evidence for no difference between them in bilateral pre-SMA. Thus, the bilateral pre-SMA did not share a similar neural code in hand movement direction across ME and MI.

MI is generally classified into two different types: kinesthetic type and visual type (Jeannerod, 1995). Our participants might unconsciously imagine the trajectory of the cursor movement while moving the joystick during the ME sessions. In the MI sessions, the participants were instructed to imagine both the visual and kinesthetic aspects of hand movement. Although visuomotor imagery was present in both ME and MI sessions, the participants might have had difficulty visualizing the hand and cursor movements simultaneously. This might be the reason why pre-SMA activation patterns were different between ME sessions and MI sessions. Additionally, whereas pre-SMA is related particularly to visuomotor imagery (Deiber et al., 1998), we cannot deny the possibility that our participants primarily used the kinesthetic type of MI during MI sessions, which might also allow pre-SMA to be decoded with significantly higher

accuracy than the chance level.

Conclusion

In summary, using multivariate analysis of fMRI activities, we found that pre-SMA was the only motor-related region related to hand movement direction in both ME and MI, but the activity patterns of ME and MI were distinct from each other.

Glossary:

motor execution, ME; motor imagery, MI; functional magnetic resonance imaging, fMRI; presupplementary motor area, pre-SMA; multivoxel pattern analysis, MVPA; representational similarity analysis, RSA; echo-planar imaging, EPI; repetition time, TR; echo time, TE; flip angle, FA; field of view, FOV; regions of interest, ROIs.

Funding: This work was supported by JSPS KAKENHI Grant Numbers JP21H00958 & JP19H00634 to K.O and JST SPRING, Grant Number JPMJSP2119 to Y.Y. This work was partially supported by Graduate Grant Program of Graduate School of Humanities and Human Sciences, Hokkaido University.

Acknowledgment: The authors would like to thank Enago (www.enago.jp) for the English language review.

Declaration of Interest: None.

References:

Brainard, D. H. (1997). The Psychophysics Toolbox. *Spatial Vision*, *10*(4), 433–436. https://doi.org/10.1163/156856897X00357

Chollet, F., Dipiero, V., Wise, R. J. S., Brooks, D. J., Dolan, R. J., & Frackowiak, R. S. J. (1991). The functional anatomy of motor recovery after stroke in humans: A study with positron emission tomography. *Annals of Neurology*, *29*(1), 63–71. https://doi.org/10.1002/ana.410290112

Cunnington, R., Iansek, R., Bradshaw, J. L., & Phillips, J. G. (1996). Movement-related potentials associated with movement preparation and motor imagery. *Experimental Brain Research*, *111*(3), 429–436. https://doi.org/10.1007/BF00228732

Cunnington, R., Windischberger, C., Deecke, L., & Moser, E. (2003). The preparation and readiness for voluntary movement: A high-field event-related fMRI study of the Bereitschafts-BOLD response. *NeuroImage*, *20*(1), 404–412. https://doi.org/10.1016/S1053-8119(03)00291-X

de Lange, F. P., Helmich, R. C., & Toni, I. (2006). Posture influences motor imagery: An fMRI study. *NeuroImage*, *33*(2), 609–617. https://doi.org/10.1016/j.neuroimage.2006.07.017

Decety, J. (1996). The neurophysiological basis of motor imagery. *Behavioural Brain Research*, *77*(1–2), 45–52. https://doi.org/10.1016/0166-4328(95)00225-1

Deiber, M.-P., Ibañez, V., Honda, M., Sadato, N., Raman, R., & Hallett, M. (1998). Cerebral Processes Related to Visuomotor Imagery and Generation of Simple Finger Movements Studied with Positron Emission Tomography. *NeuroImage*, *7*(2), 73–85. https://doi.org/10.1006/nimg.1997.0314

Ejaz, N., Hamada, M., & Diedrichsen, J. (2015). Hand use predicts the structure of representations in sensorimotor cortex. *Nature Neuroscience*, *18*(7), 1034–1040.

https://doi.org/10.1038/nn.4038

Erdfelder, E., FAul, F., Buchner, A., & Lang, A. G. (2009). Statistical power analyses using G*Power 3.1: Tests for correlation and regression analyses. *Behavior Research Methods*, *41*(4), 1149–1160. https://doi.org/10.3758/BRM.41.4.1149

Faul, F., Erdfelder, E., Lang, A. G., & Buchner, A. (2007). G*Power 3: A flexible statistical power analysis program for the social, behavioral, and biomedical sciences. *Behavior Research Methods*, *39*(2), 175–191. https://doi.org/10.3758/BF03193146

Fink, G. R., Frackowiak, R. S. J., Pietrzyk, U., & Passingham, R. E. (1997). Multiple nonprimary motor areas in the human cortex. *Journal of Neurophysiology*, *77*(4), 2164–2174. https://doi.org/10.1152/jn.1997.77.4.2164

Grush, R. (2004). The emulation theory of representation: Motor control, imagery, and perception. *Behavioral and Brain Sciences*, *27*(3), 377–396. https://doi.org/10.1017/S0140525X04000093

Hanakawa, T. (2016). Organizing motor imageries. *Neuroscience Research*, *104*, 56–63. https://doi.org/10.1016/j.neures.2015.11.003

Hanakawa, T., Dimyan, M. A., & Hallett, M. (2008). Motor Planning, Imagery, and Execution in the Distributed Motor Network: A Time-Course Study with Functional MRI. *Cerebral Cortex*, *18*(12), 2775–2788. https://doi.org/10.1093/cercor/bhn036

Hanakawa, T., Immisch, I., Toma, K., Dimyan, M. A., van Gelderen, P., & Hallett, M. (2003). Functional properties of brain areas associated with motor execution and imagery. *Journal of Neurophysiology*, *89*(2), 989–1002. https://doi.org/10.1152/jn.00132.2002

Hardwick, R. M., Caspers, S., Eickhoff, S. B., & Swinnen, S. P. (2018). Neural correlates of action: Comparing meta-analyses of imagery, observation, and execution. *Neuroscience and Biobehavioral Reviews*, *94*(December 2017), 31–44. https://doi.org/10.1016/j.neubiorev.2018.08.003

Jeannerod, M. (1995). Mental imagery in the motor context. *Neuropsychologia*, *33*(11), 1419–1432. https://doi.org/10.1016/0028-3932(95)00073-C

Jeannerod, M. (2001). Neural simulation of action: A unifying mechanism for motor cognition. *NeuroImage*, *14*(1 II), 103–109. https://doi.org/10.1006/nimg.2001.0832

Johnston, S., Leek, E. C., Atherton, C., Thacker, N., & Jackson, A. (2004). Functional contribution of medial premotor cortex to visuo-spatial transformation in humans. *Neuroscience Letters*, *355*(3), 209–212. https://doi.org/10.1016/j.neulet.2003.11.011

Kamitani, Y., & Sawahata, Y. (2010). Spatial smoothing hurts localization but not information: Pitfalls for brain mappers. In *NeuroImage* (Vol. 49, Issue 3, pp. 1949–1952). Academic Press Inc. https://doi.org/10.1016/j.neuroimage.2009.06.040

Kleiner, M., Brainard, D., & Pelli, D. (2007). What's new in Psychtoolbox-3? *Perception 36 ECVP Abstract Supplement*, *36*(0), 14. https://doi.org/10.1068/v070821

Kriegeskorte, N., Mur, M., & Bandettini, P. (2008). Representational similarity analysis - connecting the branches of systems neuroscience. *Frontiers in Systems Neuroscience*, *2*(NOV), 1–28. https://doi.org/10.3389/neuro.06.004.2008

Ledoit, O., & Wolf, M. (2003). Improved estimation of the covariance matrix of stock returns with an application to portfolio selection. *Journal of Empirical Finance*, *10*(5), 603–621. https://doi.org/10.1016/S0927-5398(03)00007-0

Leek, E. C., & Johnston, S. J. (2009). Functional specialization in the supplementary motor complex. *Nature Reviews Neuroscience*, *10*(1), 78–78. https://doi.org/10.1038/nrn2478-c1

Mayka, M. A., Corcos, D. M., Leurgans, S. E., & Vaillancourt, D. E. (2006). Three-dimensional locations and boundaries of motor and premotor cortices as defined by functional brain imaging: a meta-analysis. *NeuroImage*, *31*(4), 1453–1474. https://doi.org/10.1016/j.neuroimage.2006.02.004

Misaki, M., Kim, Y., Bandettini, P. A., & Kriegeskorte, N. (2010). Comparison of multivariate classifiers and response normalizations for pattern-information fMRI. *NeuroImage*, *53*(1), 103–118. https://doi.org/10.1016/j.neuroimage.2010.05.051

Munzert, J., Lorey, B., & Zentgraf, K. (2009). Cognitive motor processes: The role of motor imagery in the study of motor representations. *Brain Research Reviews*, *60*(2), 306–326. https://doi.org/10.1016/j.brainresrev.2008.12.024

Mur, M., Bandettini, P. A., & Kriegeskorte, N. (2009). Revealing representational content with pattern-information fMRI - An introductory guide. *Social Cognitive and Affective Neuroscience*, *4*(1), 101–109. https://doi.org/10.1093/scan/nsn044

Ogawa, K., & Imai, F. (2016). Hand-independent representation of tool-use pantomimes in the left anterior intraparietal cortex. *Experimental Brain Research*, *234*(12), 3677–3687. https://doi.org/10.1007/s00221-016-4765-7

Ogawa, K., & Inui, T. (2007). Lateralization of the Posterior Parietal Cortex for Internal Monitoring of Self- versus Externally Generated Movements. *Journal of Cognitive Neuroscience*, *19*(11), 1827–1835. https://doi.org/10.1162/jocn.2007.19.11.1827

Ogawa, K., & Inui, T. (2012). Reference frame of human medial intraparietal cortex in visually guided movements. *Journal of Cognitive Neuroscience*, *24*(1), 171–182.

https://doi.org/10.1162/jocn_a_00132

Ogawa, K., Inui, T., & Sugio, T. (2006). Separating brain regions involved in internally guided and visual feedback control of moving effectors: An event-related fMRI study. *NeuroImage*, *32*(4), 1760–1770. https://doi.org/10.1016/j.neuroimage.2006.05.012

Ogawa, K., Mitsui, K., Imai, F., & Nishida, S. (2019). Long-term training-dependent representation of individual finger movements in the primary motor cortex. *NeuroImage*, *202*(July 2018), 116051. https://doi.org/10.1016/j.neuroimage.2019.116051

Pelli, D. G. (1997). The VideoToolbox software for visual psychophysics: Transforming numbers into movies. In *Spatial Vision* (Vol. 10, Issue 4, pp. 437–442). https://doi.org/10.1163/156856897X00366

Pilgramm, S., de Haas, B., Helm, F., Zentgraf, K., Stark, R., Munzert, J., & Krüger, B. (2016). Motor imagery of hand actions: Decoding the content of motor imagery from brain activity in frontal and parietal motor areas. *Human Brain Mapping*, *37*(1), 81–93. https://doi.org/10.1002/hbm.23015

Rizzolatti, G., Fogassi, L., & Gallese, V. (2002). Motor and cognitive functions of the ventral premotor cortex. *Current Opinion in Neurobiology*, *12*(2), 149–154. https://doi.org/10.1016/S0959-4388(02)00308-2

Sanes, J., Donoghue, J., Thangaraj, V., Edelman, R., & Warach, S. (1995). Shared neural substrates controlling hand movements in human motor cortex. *Science*, *268*(5218), 1775–1777. https://doi.org/10.1126/science.7792606

Walther, A., Nili, H., Ejaz, N., Alink, A., Kriegeskorte, N., & Diedrichsen, J. (2016). Reliability of dissimilarity measures for multi-voxel pattern analysis. *NeuroImage*,

137, 188–200. https://doi.org/10.1016/j.neuroimage.2015.12.012

Weaverdyck, M. E., Lieberman, M. D., & Parkinson, C. (2020). Tools of the Trade Multivoxel pattern analysis in fMRI: a practical introduction for social and affective neuroscientists. *Social Cognitive and Affective Neuroscience*, *15*(4), 487–509. https://doi.org/10.1093/scan/nsaa057

Zabicki, A., de Haas, B., Zentgraf, K., Stark, R., Munzert, J., & Krüger, B. (2017). Imagined and executed actions in the human motor system: Testing neural similarity between execution and imagery of actions with a multivariate approach. *Cerebral Cortex*, *27*(9), 4523–4536. https://doi.org/10.1093/cercor/bhw257

Tables

Table 1: Number of ROIs' voxels in MVPA

ROI	number of voxels (SD)
left M1	925.73 (54.31)
bilateral pre-SMA	598.80 (21.67)
bilateral SMA	696.93 (10.82)
left PMv	788.20 (30.23)
left V1	457.47 (14.63)

Table 2: Training sets and test sets in multivoxel pattern classification

Training sets	number of trials	Test sets	number of trials
ME classification			
ME session 1&2	40	ME session 3	20
ME session 1&3	40	ME session 2	20
ME session 2&3	40	ME session 1	20
total	120		60
MI classification			
MI session 1&2	40	MI session 3	20
MI session 1&3	40	MI session 2	20
MI session 2&3	40	MI session 1	20
total	120		60
Cross-classification			
ME session 1,2&3	60	MI session 1,2&3	60
MI session 1,2&3	60	ME session 1,2&3	60
total	120		120

Table 3: Anatomical regions, peak voxel coordinates, and t-values of observed activations.

Anatomic region	voxels	MNI coordinates	*t*-value

		x	y	z	
Execution					
L Precentral cortex	153	−33	−28	62	12.67
Postcentral cortex		−33	−22	50	12.37
R Lingual gyrus	37	21	−79	2	12.58
Calcarine sulcus		12	-79	11	10.34
Vermis	107	3	−61	−13	11.63
R Cerebellum		21	−46	−19	9.89
L Insula	35	−39	−4	11	11.35
Rolandic operculum		-48	-1	5	9.32
L Middle occipital gyrus	13	-15	-95	-1	10.19
L Rolandic operculum	13	-45	-28	17	9.27
Imagery					
R SMA	185	12	8	65	16.33
L SMA		3	14	50	13.63
L Superior parietal lobule	44	-21	-67	53	15.04
R Inferior frontal gyrus	36	48	11	2	14.50
Insula		42	5	2	11
R Insula	33	33	26	-1	13.53
R Fusiform	79	33	−61	−10	13.05
Lingual gyrus		18	−76	−7	12.02
L Insula	90	-39	17	2	12.65
L Precentral cortex	14	-54	8	23	11.4
R Inferior frontal gyrus	16	54	11	17	10.83
L Supramarginal	21	-60	-28	38	10.62
R Precentral cortex	71	39	-13	56	10.61
L Fusiform	47	-33	-55	-16	10.44
Lingual gyrus		-21	-76	-10	9.74
L Middle frontal gyrus	18	-27	-4	53	9.64
Execution > Imagery					
L Postcentral cortex	93	-36	-31	56	13.47
Precentral cortex		-39	-19	59	8.81
Vermis	14	3	-61	-19	10.84
Imagery > Execution					
R Precentral cortex	41	36	-19	53	13.27

Execution Left					
L Precentral cortex	128	−33	−28	62	13.93
Postcentral cortex		−48	−22	53	11.04
R Lingual gyrus	25	21	−79	2	11.75
Vermis	95	3	−61	−16	10.72
R Cerebellum		18	−46	−19	10.30
L Insula	15	−42	−4	8	9.65
Execution Right					
L Postcentral cortex	144	−33	−22	50	13.00
Precentral cortex		−33	−28	59	11.82
L Insula	36	−39	−4	11	12.61
Rolandic operculum		−48	−1	5	10.35
R Cerebellum	38	33	−52	−22	10.62
Vermis	33	3	−64	−10	10.49
L Lingual gyrus	10	−12	−76	−1	9.68
Imagery Left					
R Insula	27	36	26	−1	13.23
R Inferior frontal gyrus	25	48	11	2	11.71
Insula		42	5	−1	10.49
L SMA	49	3	14	50	11.37
L Superior parietal lobule	26	−21	−67	53	11.35
L Insula	50	−36	17	2	10.52
Inferior frontal gyrus		−51	11	2	9.62
R Lingual gyrus	18	18	−76	−7	10.46
R Precentral cortex	10	36	−7	50	10.28
L Lingual gyrus	30	−21	−76	−7	10.10
Fusiform		−27	−61	−10	9.60
R SMA	10	12	8	65	10.01
R Postcentral cortex	11	48	−19	44	9.67
L Supramarginal	10	−60	−31	41	9.66
Imagery Right					
R Fusiform	149	33	−61	−10	23.91
Lingual gyrus		18	−79	−7	12.09
L Superior parietal lobule	80	−27	−61	44	15.66
R SMA	181	12	8	65	13.82
L SMA		3	14	50	13.46
L Insula	76	−33	23	8	13.59
R Precentral cortex	141	39	−10	59	13.10

Postcentral cortex		45	−22	53	10.23
L Fusiform	72	−33	−58	−16	11.87
Lingual gyrus		−18	−79	−10	10.21
L Supramarginal	24	−60	−31	38	11.77
R Insula	69	33	26	2	11.73
Inferior frontal gyrus		48	11	2	11.51
L Superior frontal gyrus	19	−21	−1	68	10.32
L Precentral cortex	16	−36	−7	41	10.32
L Inferior frontal gyrus	15	−51	11	20	9.58

MNI, Montreal Neurological Institute; L, left hemisphere; R, right hemisphere.

Figures

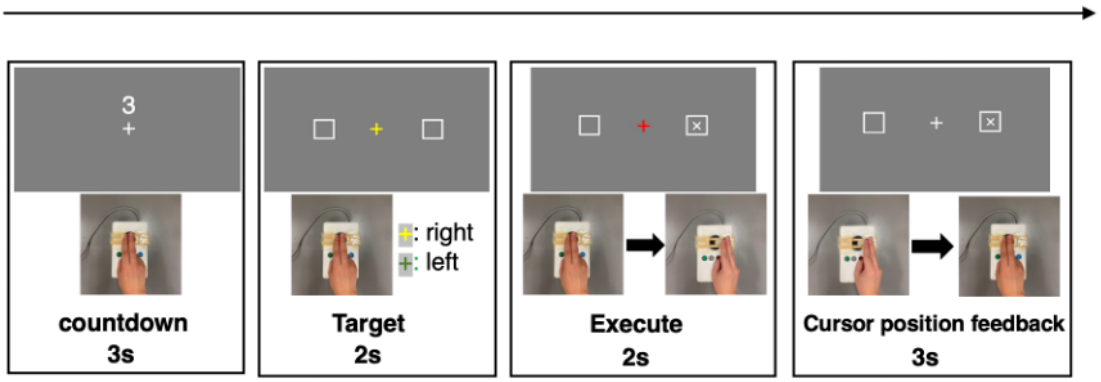

Figure 1: Schematic depiction of the time course of a single trial in the practice session. Each practice session included 10 trials. During the target phase, the order in which the colors appear in the central fixation was random, and the same color would not appear three consecutive times. The cursor is available to participants during the execution phase only during the first practice session. The joystick can only be moved to the left and right directions. Participants are instructed to move the joystick after the central fixation turns red.

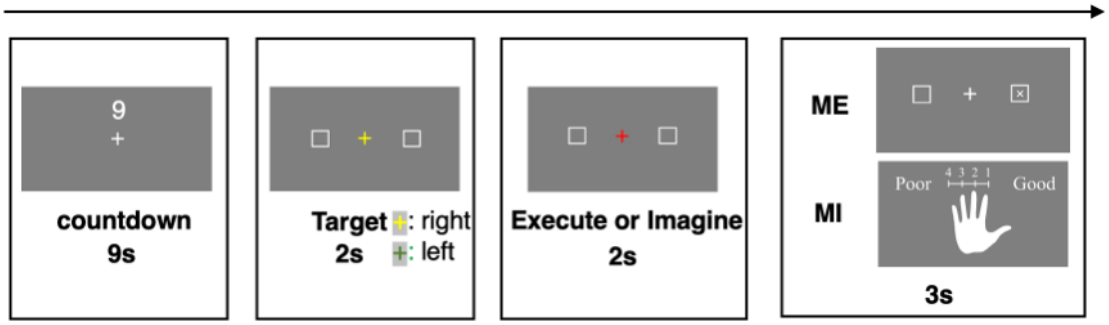

Figure 2: Schematic depiction of the time course of a single trial in ME session and MI session. Each session included 20 trials. ME session was almost the same as practice session 2, but the countdown phase changed to 9s. Participants were instructed to evaluate the quality of the imagery after the picture of the hand appeared on the screen.

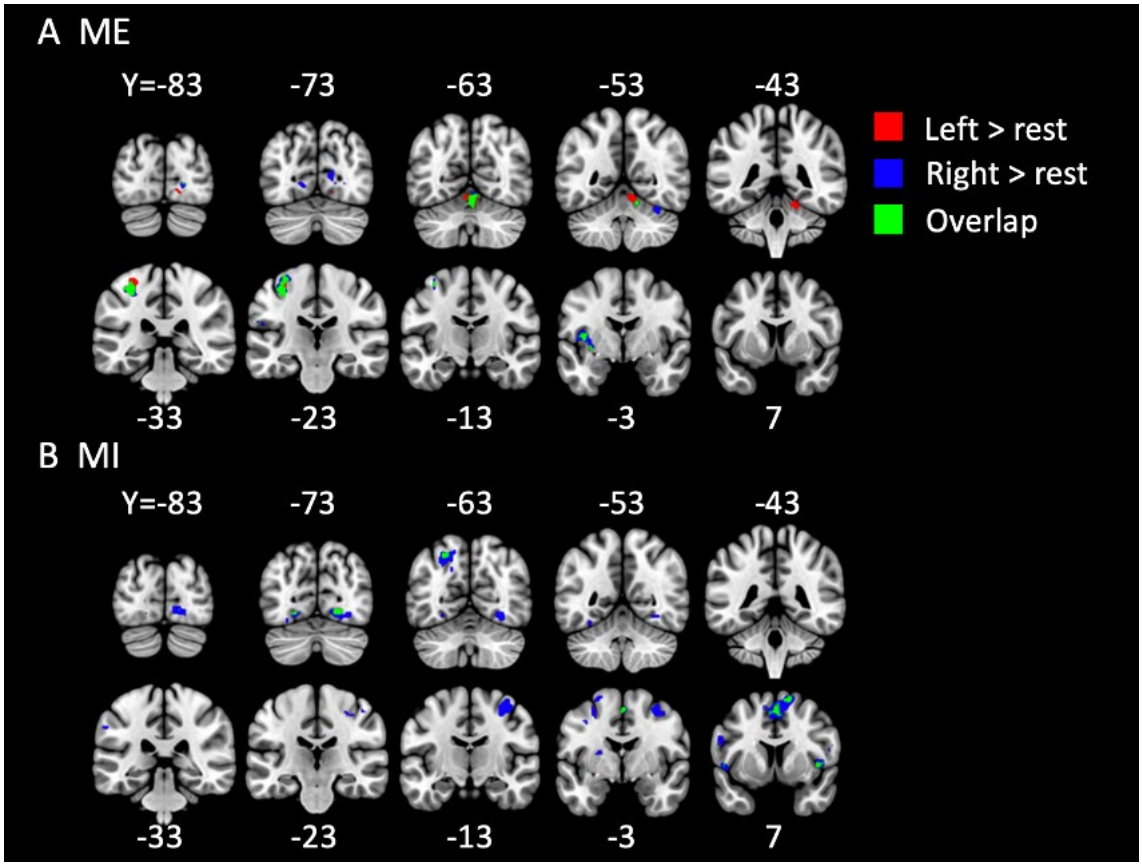

Figure 3: Activated regions in the fMRI univariate analysis of ME > rest (A) and MI > rest (B). Red showed only the left direction and blue showed only the left. Green regions were activated during both left and right directions.

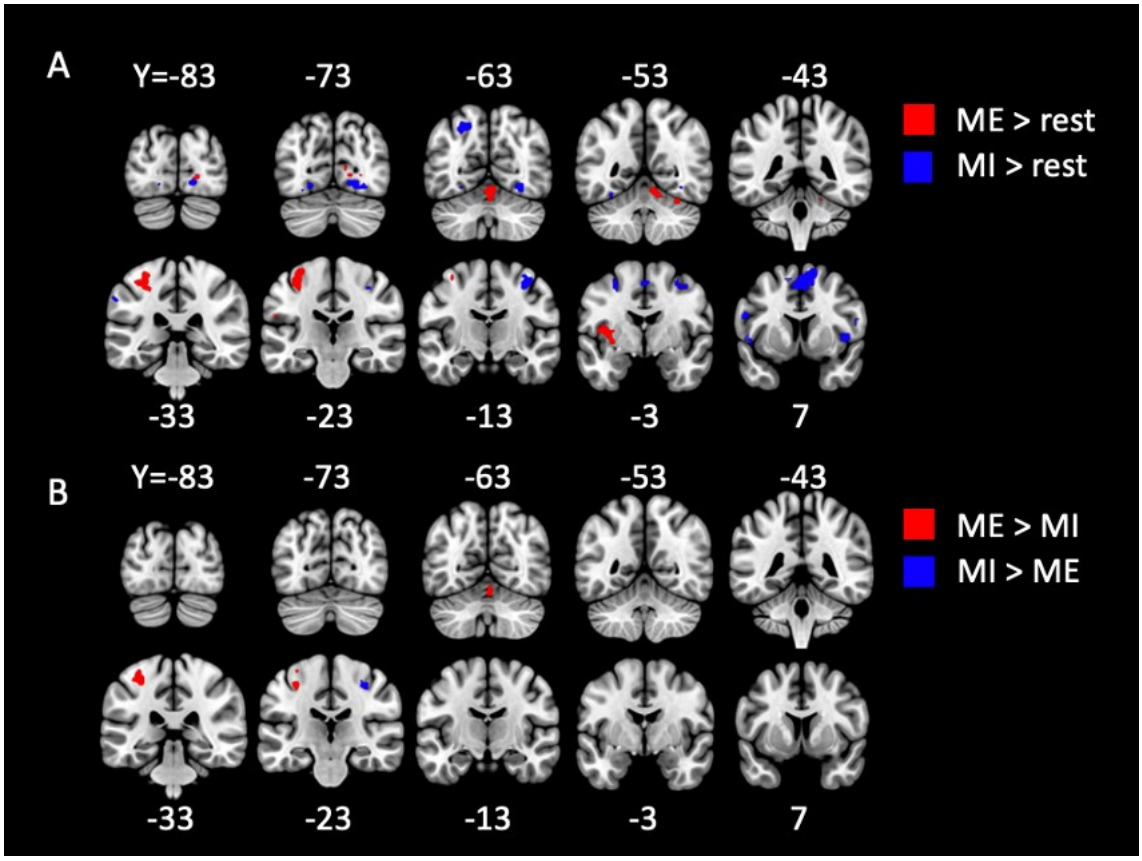

Figure 4: Activated regions in the fMRI univariate analysis of Task vs. Rest (A) and ME sessions vs. MI sessions (B).

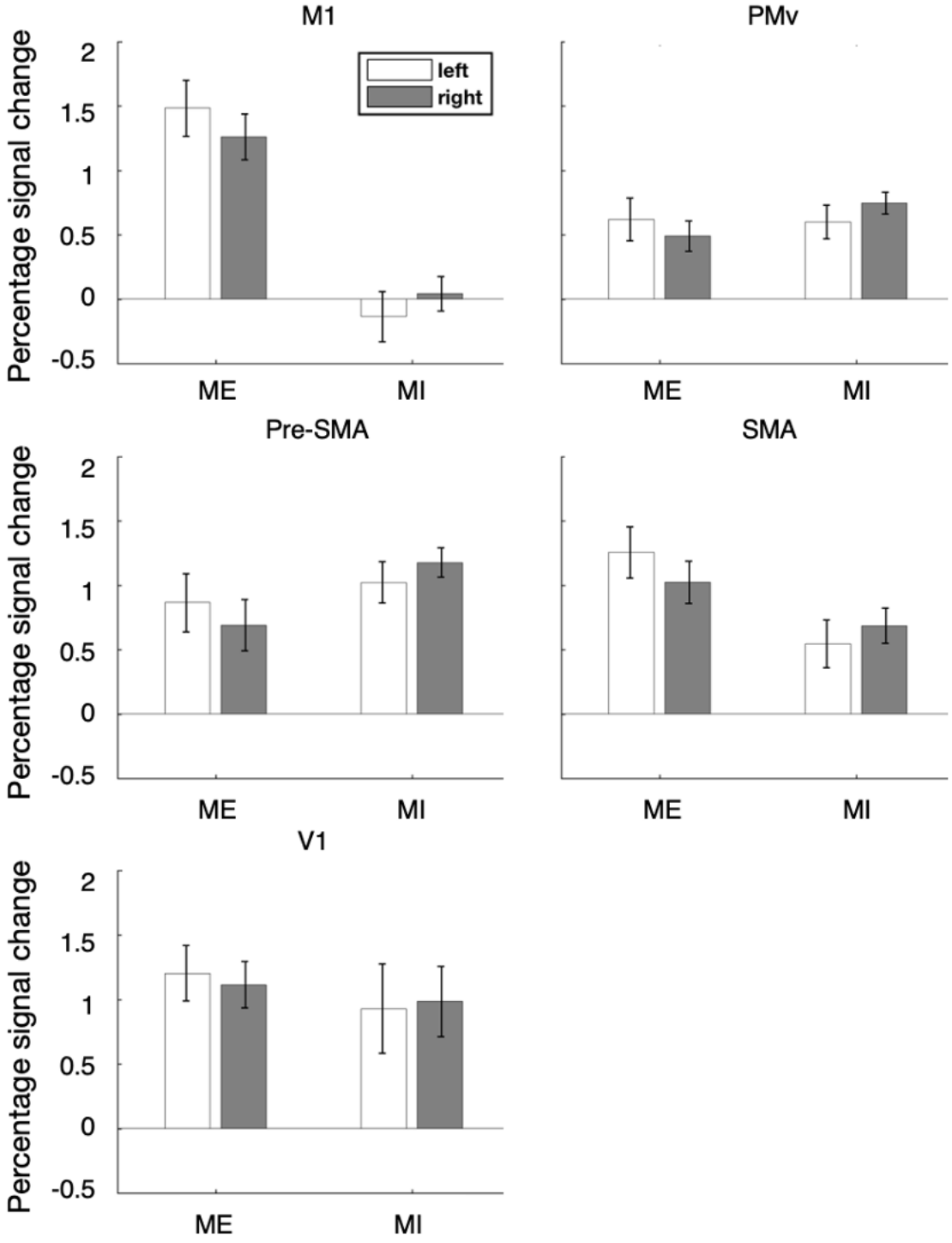

Figure 5: The averaged activation (beta value) within left M1, PMv, and bilateral pre-SMA, SMA, V1; error bars indicate SEMs.

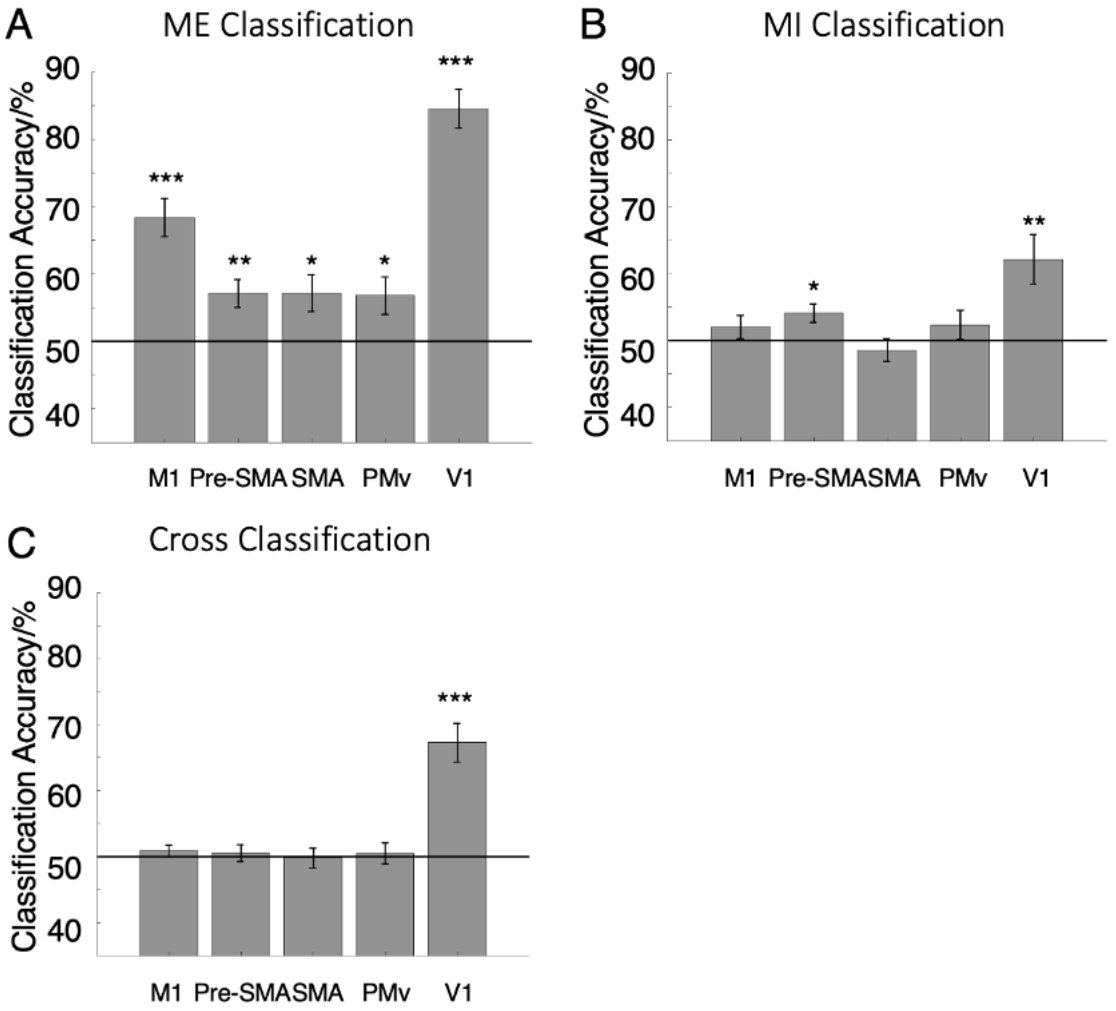

Figure 6: Classification accuracies with MVPA in ME classification (A), MI classification (B), and cross-classification (C) for movement directions in each ROI. (*p < .05, **p < .01, and ***p < .001)

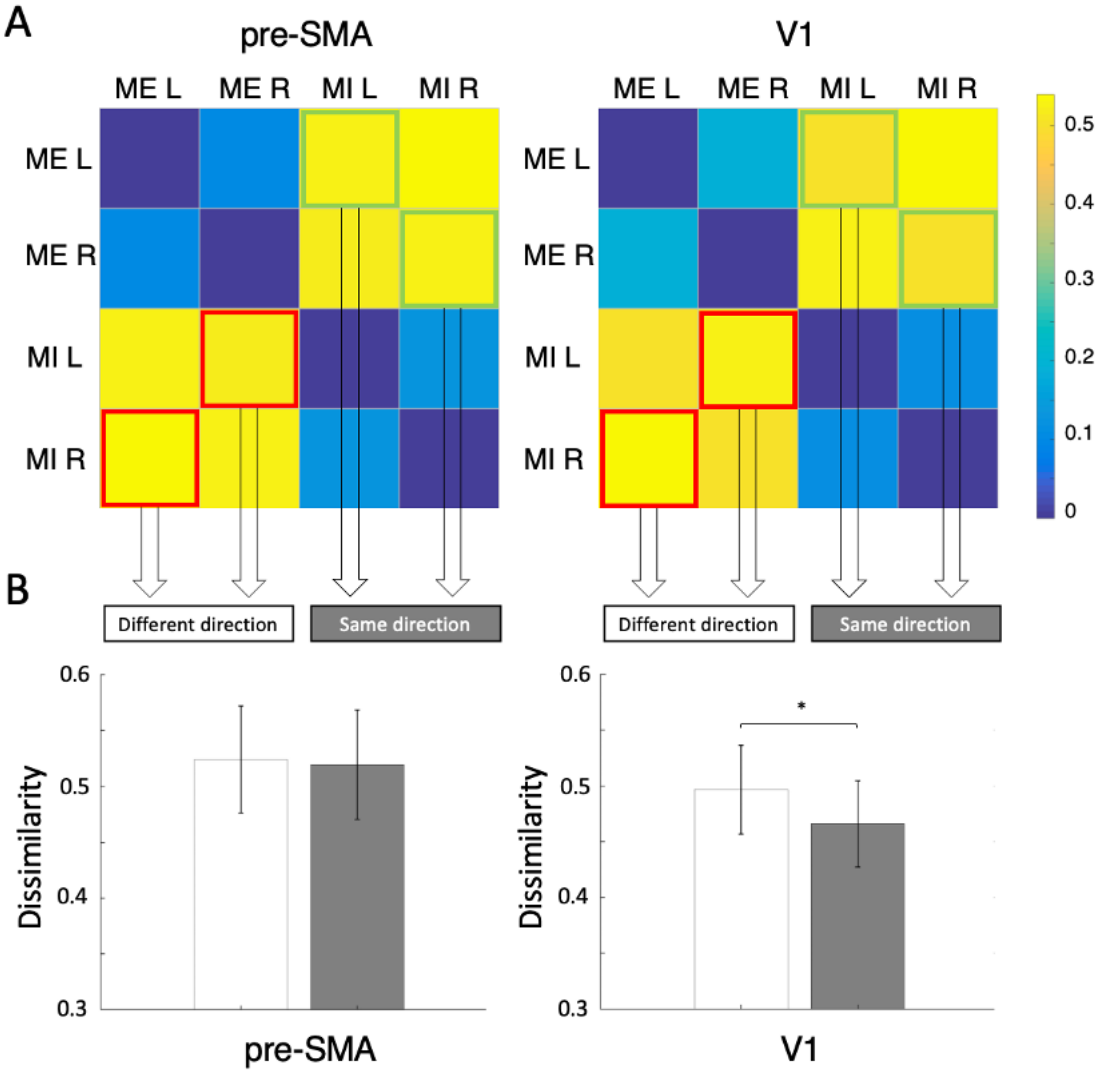

Figure 7: Representational similarity analysis (RSA) in bilateral pre-SMA and left V1. Matrix squares show the representational dissimilarity matrix between different directions and modalities, the blue rectangles show the dissimilarity between different modalities but the same direction, and the red rectangles show the dissimilarity between different modalities and different directions (A). The bar plots show the dissimilarities of the same direction and different directions between different modalities; error bars indicate SEMs (B). (*$p < .05$, **$p < .01$, and ***$p < .001$).